



HAL
open science

Sticking Properties of Water Clusters

Sébastien Zamith, Pierre Feiden, Pierre Labastie, Jean-Marc L’Hermite

► **To cite this version:**

Sébastien Zamith, Pierre Feiden, Pierre Labastie, Jean-Marc L’Hermite. Sticking Properties of Water Clusters. *Physical Review Letters*, 2010, 104 (10), pp.103401. 10.1103/PhysRevLett.104.103401 . hal-00506580

HAL Id: hal-00506580

<https://hal.science/hal-00506580>

Submitted on 28 Jul 2010

HAL is a multi-disciplinary open access archive for the deposit and dissemination of scientific research documents, whether they are published or not. The documents may come from teaching and research institutions in France or abroad, or from public or private research centers.

L’archive ouverte pluridisciplinaire **HAL**, est destinée au dépôt et à la diffusion de documents scientifiques de niveau recherche, publiés ou non, émanant des établissements d’enseignement et de recherche français ou étrangers, des laboratoires publics ou privés.

Sticking properties of water clusters

Sébastien Zamith^{1,2}, Pierre Feiden^{1,2}, Pierre Labastie^{1,2}, and Jean-Marc L'Hermite^{1,2}

¹*Université de Toulouse ; UPS ; Laboratoire collisions Agrégats Réactivité, IRSAMC ; F-31062 Toulouse, France*

²*CNRS ; UMR 5589 ; F-31062 Toulouse, France*

(Dated: July 28, 2010)

Absolute attachment cross sections of single water molecules onto mass selected protonated water clusters have been measured in the 30 – 200 size range and for collision energies down to ~ 50 meV. The major surprise is that the attachment cross sections are always smaller or equal to the hard sphere cross section. The attractive interaction between water molecules and charged water nanodroplets does not enhance the sticking probability as expected. The attachment probability is reduced due to dynamical processes on short time scale, that is, inelastic scattering occurs when the duration of the collision becomes smaller than the period of the O·O·O surface bending motion. A simple analytical expression is derived that gives the sticking probability of a water molecule onto a water nanodroplet in a vapor as a function of the vapor temperature and the size of the droplet.

PACS numbers: 36.40.-c, 36.40.Jn, 34.10.+x

Whenever a water vapor is supersaturated, such as in steam, mist, or clouds, the vapor to liquid phase transition occurs through the formation of water droplets. The first stage of growth at the molecular scale is crucial and determines the probability for what eventually become large water droplets [1]. The attachment of a single molecule onto a small droplet is the basic elementary process that determines the growth rate (also called nucleation rate). For large enough particles, sticking cross sections are very well approximated by the geometrical cross section obtained from the hard sphere (or geometric) approximation. For small particles, the range of the intermolecular forces between a single molecule and a droplet can no longer be neglected compared to the radius of the particle, and sticking cross sections are expected to become larger than hard sphere cross sections. This is particularly true when one goes from neutral to charged clusters, due to the increased attractive force of the ion-induced dipole interaction [2]. This effect has been experimentally demonstrated for sodium [3], but it cannot be generalized since intermolecular forces, thus sticking cross sections, are highly system dependent. In nucleation models, which describe the growth of droplets in a supersaturated vapor, the sticking cross sections of droplets are assumed to be equal [4, 5] or greater than that given by the hard sphere approximation, especially for charged particles [6]. The major surprise of the present study is that we arrive at the opposite conclusion. Indeed, at least under our experimental conditions, we find that the attachment cross sections of water molecules onto charged water clusters are always smaller than or equal to the hard sphere cross sections.

In this Letter, we report the measurement of the size dependence of the absolute cross sections for the attachment of water molecules onto mass-selected protonated water clusters. Apart from the cluster source, the experimental setup is nearly the same as that used to perform similar experiments on sodium clusters [3, 7]. The pos-

itively charged, protonated water clusters are produced in a gas aggregation source. Right after production they enter the thermalization stage where their temperature is set as low as possible (25 K typically). The clusters are then mass selected, energy focused and slowed down by using a novel focusing device [7]. Translational kinetic energies E_k as low as 5 eV in the laboratory frame are reached. The mass-selected clusters then enter the collision cell that contains a controlled pressure of water vapor. The pressure in the cell is monitored by both an ionization gauge (Leybold Ionivac) and a mechanical one (Leybold Ceravac CTR 91) to allow an accurate calibration of the pressure in the cell. Within the cell, the cluster ions can undergo a number of collisions, and the resulting products are mass analyzed using a time of flight mass spectrometer. Upon attachment, the energy deposited in a cluster of size n is $D + E_c$, with D the dissociation energy of the cluster of size $n + 1$ and E_c the mean collision energy in the center of mass frame:

$$E_c = \frac{E_k}{n+1} + \frac{3k_B T}{2} \frac{n}{n+1}. \quad (1)$$

In this equation, k_B is the Boltzmann constant and T the temperature of the vapor. For a cluster of a hundred molecules and for $E_k = 5$ eV, the collision energy is about 90 meV, which is only about twice the thermal kinetic energy at room temperature. The excellent transmission of the device ($\sim 50\%$) allows the study of much larger clusters than was previously possible. In particular, as a result of the poor efficiency of the velocity selection used to study low collision energies, previous experiments were limited to very small water clusters ($n \leq 11$) [8, 9]. For such small clusters, the collision energy of a sticking collision is sufficiently high to induce further evaporation. Thus, in previous experiments, the sticking cross sections cannot be measured independently of evaporation.

The sticking cross sections are deduced from the mass distribution observed after the mass selected clusters have crossed the cell [7]. Both initial temperature and

collision energy are well controlled and kept sufficiently low to avoid any evaporation due to collision-induced heating of the cluster. The arrangement allows the reliable measurement of absolute sticking cross sections without the need for any assumption concerning evaporation.

The pressure in the collision cell is set to ensure the mean number of collisions is of the order of unity. The sticking cross section is easily obtained from the number of clusters that have undergone at least one sticking collision, and is given by [3]:

$$\sigma_n = -\frac{\ln I/I_0}{l\rho} \left\{ \operatorname{erf}(\sqrt{a}) + \frac{1}{2a}\operatorname{erf}(\sqrt{a}) + \frac{e^{-a}}{\sqrt{\pi a}} \right\}. \quad (2)$$

Here, $a = E_k/(nk_B T)$, l is the length of the cell, ρ the molecular density inside the cell, n the size of the incoming cluster, T the temperature of the vapor, and erf is the error function. I_0 is the total number of incoming clusters whereas I is the number of clusters that have undergone no sticking collisions. The first term on the right side of Eq. 2 comes from the standard Beer-Lambert law, while the term inside the braces accounts for the thermal distribution of translational energies of the impinging molecules. The main uncertainty in the cross section measurement comes from the determination of the gas density in the cell. We estimate the uncertainty of the pressure measurement to be on the order of 20%.

Even after being heated by the sticking collision, the lifetime of the clusters under our experimental conditions is much larger than the time of flight in the second mass spectrometer. The absence of evaporation has been verified by measuring the variation of the experimental cross section as a function of the initial temperature of the clusters. When the internal energy is high enough to induce evaporation before the detector, the measured sticking cross section drops abruptly. The temperature at which this drop occurs depends slightly on the size, but is always far above 100 K, whereas in the present measurement our clusters are thermalized at a temperature of 25 K.

The cross sections for the attachment reactions $(H_2O)_n H^+ + H_2O \rightarrow (H_2O)_{n+1} H^+$ have been measured at five kinetic energies in the lab frame, $E_k=6,10,18,22$ and 33 eV. The evolution of the sticking cross sections as a function of the cluster size is shown in figure 1, along with the hard sphere cross section (full line in Fig. 1). The hard sphere cross section is calculated as $\sigma_{geo} = \pi(R_{cluster} + r_{molecule})^2$, with $R_{cluster} = r_{molecule}n^{1/3}$. We used $r_{molecule} = 2.25 \text{ \AA}$ (the molecular radius deduced from the density of ice is about 2 \AA). The most noticeable features are the decrease of the cross section as the collision energy increases and as the size decreases. As deduced from Eq.1, these features are correlated because at constant laboratory kinetic energy, the collision energy in the center of mass frame increases as the size decreases. For cluster sizes above $n \sim 100$, the cross sec-

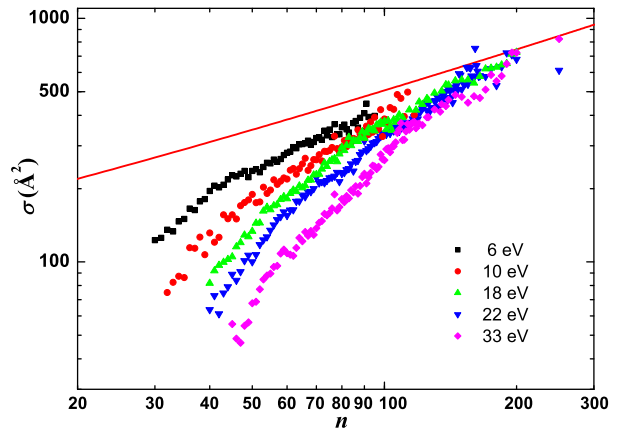


FIG. 1. (color online) Log-Log plot of the sticking cross section as a function of cluster size for five different kinetic energies in the lab frame. Experimental results are compared to the hard sphere model (full line).

tions converge nicely toward the hard sphere approximation. Deviation from geometrical cross sections at small sizes has been predicted for neutral reagents [10] and experimentally observed in the sticking of sodium atoms onto positively charged sodium clusters. Quite surprisingly, however, the cross section for water never exceeds the hard sphere cross section, even at the lowest kinetic energy collision. Sticking cross sections of sodium atoms onto sodium clusters are significantly higher than hard sphere cross sections at low collision energy, which is qualitatively understood in terms of a model based on a charge-induced dipole interaction [3]. Water clusters not only interact with water molecules through charge-induced dipole interaction, but also through the charge-permanent dipole interaction, both of which are attractive forces. Furthermore, the attractive short range interaction is expected to result in an enhancement of the sticking cross section [11], especially at small size and low collision energy [12]. However, no evidence for such an enhancement has been observed in our experiment, and in fact the opposite behavior has been observed. In the following we will examine different hypotheses that could explain this small cross-section.

To check the influence of possible exchange collisions, where a molecule of the cluster is replaced by the impinging one, experiments have been conducted where the target molecules H_2O have been replaced by heavy water molecules D_2O . Water/heavy water exchange reactions $(H_2O)_n H^+ + D_2O \rightarrow (H_2O)_{n-1} (D_2O) H^+ + H_2O$ are indeed observed (see figure 2). The single proton/deuterium exchange leading to products $(H_2O)_n (HDO) H^+$ also appear as weak features in our mass spectra. Such results have also been observed in low energy collisions of heavy water and small protonated water clusters [9]. The ratio of exchange to attachment probability is deduced from the areas of the correspond-

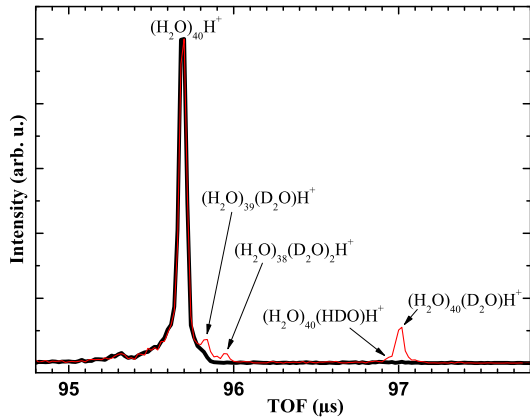


FIG. 2. (color online) Mass spectra resulting from the collision of $(H_2O)_{40}H^+$ with D_2O at a kinetic energy of 22 eV in the lab frame ($E_c = 0.57$ eV). The thick black curve corresponds to no vapor in the cell, whereas the thin curve (red online) corresponds to a water vapor density of $3.4 \cdot 10^{18}$ molecules/ m^3 in the cell. Evidence for exchange reactions is clearly visible.

ing peaks in mass spectra such as the one of figure 2. The observed cross sections for the exchange reaction are not sufficiently high to account for the difference between geometrical and observed cross sections. For example, at 22 eV, the exchange would only raise the cross section for $(H_2O)_{40}H^+$ from 60 \AA^2 to 100 \AA^2 , still far below the geometrical cross section (280 \AA^2). Furthermore, as the cluster size increases and/or the collision energy decreases, the exchange reaction becomes increasingly less important, and is completely negligible for $n > 60$ and 22 eV.

The systematic decrease of the sticking cross section is observed over an extended size range, and varies smoothly with the size. This feature suggests that the reduction of cross sections does not result from the possible non spherical shape of some clusters. Moreover, fragmentation cross sections have been measured at higher kinetic energy in the lab frame, ranging from 70 eV to 400 eV and for sizes as small as $n = 40$. As expected [13], they do converge toward spherical geometrical cross sections.

Charge exchange might also open quenching channels leading to non sticking collisions. One possible output channel is $(H_2O)_{n+1} + H^+$, whose energy lies above the entrance channel by approximately $PA((H_2O)_n) - HE((H_2O)_n)$, where PA is the proton affinity and HE the hydration energy. In the present case, $PA \sim 9$ eV [14, 15] and $HE \sim 0.5$ eV [14, 16]. Thus, this channel is inaccessible in our experiments, where the collision energy in the center of mass frame is always much less than 1 eV. Another possible quenching channel would produce $(H_2O)_n + H_3O^+$. These products lie above the energy of the entrance channel by the quantity $PA - D(H_3O^+)$, where $D(H_3O^+)$ is the dissociation energy of the pro-

cess $H_3O^+ \rightarrow H_2O + H^+$, or 7.22 eV [17]. Thus the neutralization channel $(H_2O)_n + H_3O^+$ lies at least at 1.78 eV above the entrance channel, and is also not energetically allowed. In short, charge exchange reactions cannot account for the low sticking cross sections measured at small sizes.

The decrease of cross sections is probably due to inelastic scattering where the impinging molecule bounces off the cluster without being trapped in its potential. As indicated above, we have checked that the clusters do not evaporate due to thermal decay. Thus, non-reactive collisions are likely because direct collisions do not form collision complexes with sufficient lifetimes to ensure internal vibrational energy redistribution (IVR). In particular, collision complexes are formed when the duration of the collision is longer than the time required for the excess energy to be redistributed among the internal degrees of freedom of the complex. Such events, for which attachment is successful, can be described as adiabatic. During sudden collisions, the impinging molecule essentially interacts with a single molecule of the cluster, which undergoes a strong collisional energy transfer. The adiabaticity parameter, $\xi = \tau_c/\tau_v$, where τ_c is the duration of the collision and τ_v a relevant vibrational period of the target, can be introduced to separate adiabatic from sudden regimes [18]. Large ξ values lead to attachment whereas small values, for which a large translational momentum is instantaneously transferred to a single molecule from the cluster, lead to inelastic collisions in which either the impinging molecule just bounces off the cluster, or a molecule is ejected from the cluster and replaced by the impinging molecule. In our experiment, the duration of the collisions τ_c is estimated by the time needed to cover a distance of the order of the diameter of the cluster. Thus, the collision time as a function of size and kinetic energy in the lab frame is given by:

$$\tau_c = 2n^{1/3}r(2E_k/(nm) + 3k_B T/m)^{-1/2} \quad (3)$$

Here m and r are the mass and radius of a single water molecule, respectively. The probability for undergoing an inelastic collision can be estimated by using the hard sphere cross section, σ_{geo} , and the expression $P_{inelastic} = (\sigma_{geo} - \sigma_{exp})/\sigma_{geo}$. This value is plotted in figure 3 as a function of τ_c for all of the current experimental data. The nice overlap of all curves corresponding to different collision energies and different sizes suggests that the adiabaticity parameter is the relevant quantity here. The good agreement of Figure 3 cannot be obtained when plotting $P_{inelastic}$ as a function of any other parameter, such as the collision energy for instance.

The probability of undergoing an inelastic collision decreases exponentially with τ_c . The best fit by a function $e^{-(\tau_c - \tau_0)/\tau_v}$ gives a characteristic time $\tau_v = 0.75$ ps, which corresponds to a vibrational energy of 5.6 meV. This value is in excellent agreement with the energy of the $O \cdots O \cdots O$ bending mode (5.1 meV) [19], which is the

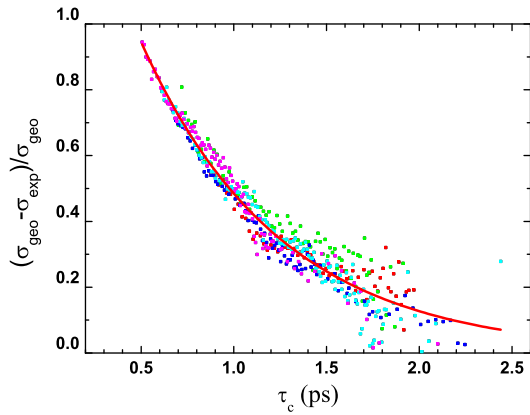


FIG. 3. Probability of inelastic collision as a function of the collision duration. Each point corresponds to a different value of the cluster size and/or collision energy. The full line is an exponential fit to the data (see text for details).

principal low-energy surface vibrational mode excited by collisions. The excellent agreement between the vibrational period of the O··O··O bending motion and the characteristic collision time suggests that there is a close relation between the sticking probability and the ratio of the duration of the collision to the period of the surface intermolecular vibration, as expected in the adiabatic versus sudden model [18]. Dynamical effects and the timescale of IVR processes have already been shown to play a significant role in promoting or inhibiting the reactivity of small clusters [20]. The collision energy range investigated in this work is a little higher than the mean thermal collision energy in a vapor. Nevertheless our lowest collision energies are only twice the average thermal collision energy at 273 K. Strikingly, even at this low energy, no evidence has been observed for enhanced attachment resulting from the long range interaction between the cluster and the molecule, although such an enhancement certainly occurs at very low collision energy. Thus, neglecting the long range interaction, one can extrapolate our observation to estimate the effect of fast dissociation on the sticking cross section for droplets in a vapor. The sticking efficiency $\chi = (1 - P_{inelastic})$ can be defined as a correction to the geometric sticking cross section. Assuming that the collision energy is the mean value in the canonical ensemble, χ is given by a very simple functional expression for a water nanodroplet made of n water molecules in a vapor at temperature T :

$$\chi = \sigma_{sticking} / \sigma_{geo} = 1 - e^{-(\tau_c - \tau_0) / \tau_v}, \quad (4)$$

where $\tau_c = 12n^{5/6} / \sqrt{T(1+n)}$ ps, $\tau_0 = 0.46$ ps, $\tau_v = 0.75$ ps and T is the temperature of the vapor in Kelvin.

The sticking efficiency of water is significantly reduced for small sizes, *e.g.* $\chi = 80\%$ for $n = 13$ at $T = 293$ K.

In conclusion, we have measured absolute sticking cross sections of water molecules onto protonated water clusters. Surprisingly, we find that the cross section never exceeds the geometrical cross section. We believe this result arises from dynamical effects: if the duration of the collision is too short, the cluster does not have enough time to convert the collision energy into its vibrational modes, and the sticking probability is reduced.

We gratefully acknowledge J. Vigué for stimulating discussions and S.T. Pratt for critical reading of the manuscript.

-
- [1] M. Kulmala, *Science*, **302**, 1000 (2003).
 - [2] A. B. Nadykto and F. Yu, *Phys. Rev. Lett.*, **93**, 016101 (2004).
 - [3] F. Chirot, P. Labastie, S. Zamith, and J.-M. L’Hermite, *Phys. Rev. Lett.*, **99**, 193401 (2007).
 - [4] D. W. Oxtoby, *J. Phys.: Condens. Matter*, **4**, 7627 (1992).
 - [5] I. Ford, *Phys. Rev. E*, **56**, 5615 (1997).
 - [6] S. M. Kathmann, G. K. Schenter, and B. C. Garrett, *Phys. Rev. Lett.*, **94**, 116104 (2005).
 - [7] F. Chirot, S. Zamith, P. Labastie, and J.-M. L’Hermite, *Rev. Sci. Instrum.*, **77**, 063108 (2006).
 - [8] Y. Okada, S. Yamaguchi, Y. Kawai, T. Orii, and K. Takeuchi, *Chem. Phys.*, **294**, 37 (2003).
 - [9] S. Yamaguchi, S. Kudoh, Y. Okada, T. Orii, and K. Takeuchi, *Chem. Phys. Lett.*, **359**, 480 (2002).
 - [10] J. Vigué, P. Labastie, and F. Calvo, *Eur. Phys. J. D*, **8**, 265 (2000).
 - [11] A. B. Nadykto and F. Yu, *J. Geophys. Res.*, **108**, 4717 (2003).
 - [12] T. Orii, Y. Okada, K. Takeuchi, M. Ichihashi, and T. Kondow, *J. Chem. Phys.*, **113**, 8026 (2000).
 - [13] H. Udseth, H. Zmora, R. Beuhler, and R. Friedman, *J. Phys. Chem.*, **86**, 612 (1982).
 - [14] T. F. Magnera, D. E. David, and J. Michl, *Chem. Phys. Lett.*, **182**, 363 (1991).
 - [15] R. Knochenmuss and S. Leutwyler, *The Journal of Chemical Physics*, **91**, 1268 (1989).
 - [16] Z. Shi, J. V. Ford, S. Wei, and J. A. W. Castleman, *J. Chem. Phys.*, **99**, 8009 (1993).
 - [17] F. D. Giacomo, F. A. Gianturco, F. Raganelli, and F. Schneider, *J. Chem. Phys.*, **101**, 3952 (1994).
 - [18] R. Levine and R. Bernstein, *Molecular Reaction Dynamics and Chemical Reactivity* (Oxford University Press, 1987).
 - [19] J. Brudermann, P. Lohbrandt, U. Buck, and V. Buch, *Phys. Rev. Lett.*, **80**, 2821 (1998).
 - [20] R. Mitrić, C. Bürgel, and V. Bonačić-Koutecký, *Proc. Natl. Acad. Sci. U.S.A.*, **104**, 10314 (2007).